Hydrological Sciences Journal – Journal des Sciences Hydrologiques, 60 (6) 2015
http://dx.doi.org/10.1080/02626667.2014.905690

Seasonal and inter-annual variability of water quality in the Uruguay River, Argentina

Juan C. Colombo[1,2], Carlos N. Skorupka[1], Claudio Bilos[1], Leandro Tatone[1,3], Natalia Cappelletti[1,3], M. Carolina Migoya[1,3], Malena Astoviza[1,3] and Eric Speranza[1,3]

[1]*Laboratorio de Química Ambiental y Biogeoquímica (LAQAB), Facultad de Ciencias Naturales y Museo, Universidad Nacional de La Plata, Florencio Varela, Buenos Aires, Argentina*
laqab@fcnym.unlp.edu.ar

[2]*Comisión de Investigaciones Científicas, Provincia de Buenos Aires (CIC), La Plata, Buenos Aires, Argentina*

[3]*Consejo Nacional de Investigaciones Científicas y Técnicas (CONICET), Ciudad Autónoma de Buenos Aires, Argentina*

Received 10 April 2013; accepted 12 March 2014

Editor Z.W. Kundzewicz

Abstract Water quality of the Uruguay River was evaluated with multi-parametric (temperature, turbidity, conductivity, pH, dissolved oxygen) and sediment trap data (particle flux, total organic carbon and nitrogen contents) and correlated to precipitation, river discharge and El Niño Southern Oscillation (ENSO) indices for the period 2006–2011. Hydro-meteorological parameters averaged 24–85% variability with coincident precipitation (200–400 mm month^{-1}), discharge (7000–28 000 m^3 s^{-1}) and turbidity peaks (50–80 NTU) in the austral spring, and absolute maxima during the El Niño 2009 episode. Spectral analysis of discharge and sea-surface temperature anomaly (SSTA) showed consistent variance maxima at approx. 3 and 1.5 years. Deseasonalized discharge was significantly correlated to SSTA. During river floods, pH decreased (from 7.5 to 6.6) and particle dynamics peaked (turbidity: 15–80 NTU; vertical fluxes: 20–200 g m^{-2} d^{-1}; total solid load: <1000 to 100 000 t d^{-1}),whereas TOC remained stable (3.2 ± 0.8%) and C/N ratios increased (10–12) due to the higher contribution of terrestrial detritus.

Key words ENSO; water quality; Uruguay River

Variabilité saisonnière et interannuelle de la qualité de l'eau du fleuve Uruguay, en Argentine

Résumé La qualité de l'eau du fleuve Uruguay a été évaluée avec des données multi-variables (température, turbidité, conductivité, pH, oxygène dissous) et des données de pièges à sédiments (flux de particules, teneurs en carbone et azote organiques), corrélées aux précipitations, aux débits et aux indices ENSO pour la période 2006–2011. Les variables hydrométéorologiques ont montré des moyennes de variabilité de 24 à 85%, analogues pour les précipitations (200–400 mm mois^{-1}), les débits (7000–28 000 m^3 s^{-1}) et les pics de turbidité (50-80 NTU) au cours du printemps austral, et des maximums absolus pendant l'épisode El Niño de 2009. L'analyse spectrale du débit et de l'anomalie de température de surface de la mer (ATSM) a montré des maximums de variance cohérents pour des durées de 3 et 1,5 années environ. Le débit désaisonnalisé était significativement corrélé à l'ATSM. Pendant les inondations, le pH a diminué (de 7,5 à 6,6) et la dynamique des particules a connu un pic (turbidité : 15–80 NTU; flux verticaux : 20–200 g m^{-2} jour^{-1} ; charge solide totale : <1000 à 100 000 t jour^{-1}), alors que le carbone organique total est resté stable (3,2 ± 0,8%) et que les rapports C/N ont augmenté (10–12) en raison de la contribution plus élevée de détritus terrestres.

Mots clefs ENSO ; qualité de l'eau ; fleuve Uruguay

1 INTRODUCTION

Located in southern South America, the Río de la Plata Basin is the second largest in the continent covering more than 3 × 10^6 km^2 in Argentina, Uruguay, Brazil, Paraguay and Bolivia (Esteves *et al.* 2000; Fig. 1). More than 200 million inhabitants are concentrated in the area, including the densely populated cities of San Pablo, Buenos Aires, Asunción and Montevideo, and economic activity is considerable: >80% of the GNP of the five countries (Almeira and Scian 2006). The two major tributaries of the Basin are the Paraná (3800 km) and Uruguay Rivers (1800 km) which

Fig. 1 Río de la Plata Basin indicated by the shaded area covering Argentina, Uruguay, Brazil, Paraguay and Bolivia with major rivers, cities and hydroelectric dams along the upper and lower Uruguay River. The insert shows the study area with sampling stations in the Gualeguaychú-Fray Bentos region of the Uruguay River.

together discharge to the Río de la Plata estuary about 500–800 km^3 of freshwater and 90 × 10^9 t of suspended solids per year (Degens *et al.* 1991). Hydrological parameters of both rivers display considerable monthly, inter-annual and decadal variability related to regional and global processes, i.e. a 2–7 year river flow oscillation in phase with El Niño Southern Oscillation (ENSO), with high discharges during El Niño events (EN) and low-normal flow during La Niña (LN; Depetris and Kempe 1990, Robertson and Mechoso 1998, Camilloni and Barros 2003, Krepper *et al.* 2003, Cardoso and Silva Dias 2006, Pasquini and Depetris 2007, 2010). A long-lasting (>1 year) once-in-a-century flood produced by exceptionally heavy rains, related to the warm ENSO episode of 1982/83, extensively affected the region producing massive population evacuations and huge economic losses (Depetris and Kempe 1990, Camilloni and Barros 2003). To assess the variability and anticipate these natural episodes, several oceanic and near-global atmospheric indices have been validated as predictors of rainfall and river discharge in the Río de la Plata Basin, i.e. the southern oscillation index (SOI) and sea-surface temperature anomaly (SSTA; Camilloni and Barros 2003, Almeira and Scian 2006). Conversely, since watersheds integrate all components of the water cycle (i.e. precipitation, evapotranspiration influenced by topography and vegetation cover, human effects), the discharge of the world's largest rivers constitutes a useful proxy to assess global warming and climate change trends (Labat 2008).

In this paper, we study the seasonal variability and the inter-annual influence of ENSO episodes on river discharge, water quality parameters, settling material and mass transport rates of the Uruguay River over a 6-year period.

2 STUDY AREA

The Uruguay River originates in Brazil at the confluence of the Canoas and Pelotas rivers at approx. 1800 m a.s.l. With a total drainage area of 365 000 km^2 it constitutes the natural limit between Argentina-Brazil (upper) and Argentina-

Uruguay (lower). The Uruguay River has a very irregular hydrological regime characterized by a mean flow of approx. 4000–5000 m^3 s^{-1} (García and Vargas 1998, Krepper *et al.* 2003; Fig. 1), low flows in summer, and large winter discharges and wide-ranging extreme historical flows (<100 to 35 000 m^3 s^{-1}). The delay between precipitation and discharge of the river is short (Barros *et al.* 2005). As the slope is pronounced (0.086 m km^{-1}) floods produced by intense rains are rapid and concentrated on small areas. The hydrological regime of the Uruguay River is regulated by three dams, two operated by Brazil in the upper river (Itá: 27°16.678′S–52°22.977′W, Machadinho: 27°31.548′S–51°47.131′W) and one by Argentina-Uruguay 200 km upstream of our sampling sites (Salto Grande: 31°16.5′S–57°56.344′W; Fig. 1). The Salto Grande plain dam, constructed in 1979, has a total reservoir surface area of 1500 km^2, an average depth of only 6.4 m and a low annual residence time (approx. 25 d). In combination, these factors limit the regulation capability of the dam, especially during high waters as is shown by the Salto Grande discharge/Uruguay River flow regressions (Fig. 2). Statistics display a high general slope and correlation (slope: 0.91; R^2: 0.88), with increasing values for larger river flows. The driest (2006)-wettest (2009) year pair (2106 ± 1597 *vs* 6379 ± 6664 m^3 s^{-1}) shows the greatest contrast both for the slopes (0.80–0.97) and regression significance (R^2: 0.62–0.95), reflecting reduced regulation at high water regimes.

Published information on the hydrology and water quality of the Uruguay River is fragmentary, especially when compared to the Paraná River. Periodical reports on navigation, algae blooms and fisheries surveys are published locally by the Bi-national (Argentina-Uruguay) Technical Commission of the Salto Grande Dam (CTM), and Uruguay River Administrative Commission (CARU), but well circulated, international reports are very scarce. A global study of the biogeochemistry of major world rivers, which incidentally mentions the Uruguay River (Degens *et al.* 1991), provides a general comparison with the Paraná River in terms of: water discharge, which is on average three-times lower in the Uruguay River (4500 *vs* approx. 15 000 m^3 s^{-1}); dissolved solids mass transport rate, which is six-times lower (6 *vs* 38 × 10^6 t $year^{-1}$); and total suspended solid mass transport, which is eight-times lower in the Uruguay River (11 *vs* 80 × 10^6 t $year^{-1}$ in the Paraná).

3 MATERIAL AND METHODS

3.1 Sampling

Field sampling was carried out between September 2006 and December 2011 in weekly, fortnightly and monthly field surveys along the Argentinean coast of the Uruguay River close to Gualeguaychú (Argentina) and Fray Bentos (Uruguay) cities (Fig. 1). During each sampling campaign basic water quality data (temperature, dissolved oxygen, turbidity, pH) were measured *in situ* at

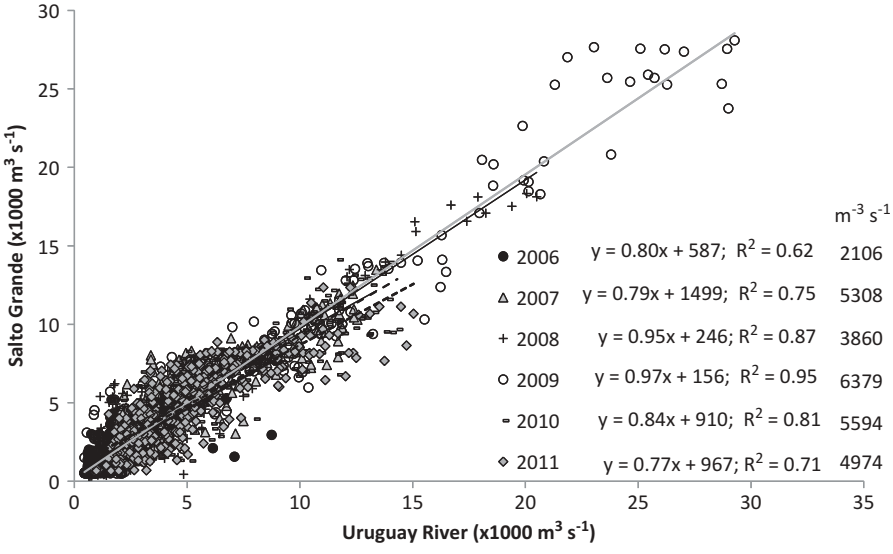

Fig. 2 Regressions of daily Salto Grande Dam discharge with Uruguay River flow for the six years covered in this study. Statistics and average river flow are indicated.

approx. 0.5 m depth from a pneumatic boat utilizing a Manta Eureka monitoring probe (Austin, TX, USA) equipped with a portable field display. In addition, from May 2008 to March 2009, other probes were moored in two fixed buoys along the river mainstream (33°06.501′S–58°20.556′W and 33°06.043′S–58°17.864′W; Fig. 1). These probes were programmed to collect water quality data every 30–60 min; these data were then used to calculate daily averages. Before measurement and deployment, the probes were calibrated in the laboratory, with subsequent confirmation in the field, using standardized procedures and certified reference solutions (Hanna Instruments, Woonsocket, RI, USA). In order to obtain a time-integrated sample of settling material, 10-cm diameter mono-cylindrical sediment traps (total surface: 78.5 cm^2), which intercept the vertical particulated flux (Colombo *et al.* 2005, 2007), were deployed for 15–30 days in the buoys; a total of 100 sediment trap samples were collected.

3.2 Chemical analysis

The material collected by the traps was centrifuged, weighed for the calculation of total mass flux, and split for the determination of water content (24 h at 100°C) and total organic carbon (TOC) and total nitrogen (TN) content, by catalytic high temperature combustion utilizing a Thermo Finnigan, CE FlashEA 1112 elemental analyser calibrated with Acetanilide OAS (71.09% C and 6.70% N; Elemental Microanalysis). The TOC/TN method accuracy and precision was evaluated through the analysis of certified reference materials: a low organic content soil standard (B2152: 1.52% TOC and 0.13% TN) and a high organic content sediment standard (B2150: 6.10% C and 0.46% N, both from Elemental Microanalysis Ltd). Average recoveries were 101 ± 2.1–102 ± 1.3% TOC and 103 ± 11–99 ± 8.2% TN, respectively. Duplicate and triplicate analysis of the trap material (typically 40 mg dry weight) resulted in relative standard deviations of 9–10%.

3.3 Database sources and statistical analysis

The freshwater discharge of the Uruguay River was calculated as the turbinated plus compensation flow discharged daily by the Salto Grande Dam (wholesale electricity market administration company: www.cammesa.com). Precipitation data were obtained for six fixed stations located in Argentina along the Uruguay River, upstream of the field sampling sites from the integrated hydrological database of the National Hydro-meteorological Network (http://www.hidricosargentina.gov.ar/sistema_sistema.php). ENSO-indices, namely the meteorological southern oscillation index (SOI), defined as the normalized pressure difference between Tahiti and Darwin, Australia, and oceanographic sea-surface temperature anomaly data for region 3.4 (SSTA), were obtained from the Climate Prediction Centre, National Weather Service of the National Oceanic & Atmospheric Administration (NOAA; http://www.cpc.ncep.noaa.gov/data/indices).

Basic statistical analyses were performed using XLSTAT version 2011.2.08. The inter-annual variability was evaluated by Fourier spectral analysis (SPSS 19.00). Deseasonalizing of freshwater discharges was carried out by dividing the original data by the seasonal index (SI), obtained for each month from the quotient of monthly values divided by the order-12 moving average of the corresponding month.

4 RESULTS

Figure 3 presents the variation of daily freshwater discharge, the accumulated monthly precipitation (plotted at the end of each month), temperature and turbidity measured at different time intervals (daily to monthly) from 2006 to 2011. ENSO indices (SOI and SSTA) are also presented at the top of the figure with major episodes indicated by solid-black (warm, i.e. El Niño) and dashed-grey arrows (cold, La Niña), which are also identified in the time scale (month 3, 6, 9 and 12 for each year).

Hydro-meteorological parameters display average 24–85% variability; temperature reflects the winter–summer seasonality (12–28°C) and displays lower variability (average: 20 ± 5°C, or ±24% variability); the freshwater discharge fluctuate from 307 to 28 091 $m^3\ s^{-1}$ (4659 ± 3960 $m^3\ s^{-1}$, ±85%), the monthly precipitation ranges from 12 to 429 mm $month^{-1}$ (77 ± 59 mm $month^{-1}$, ±59%) and turbidity from 5 to 83 NTU (28 ± 14 NTU, ±50%). ENSO indices show higher >100–200% variability; SOI ranged from –2.4 to 4.8 (1.1 ± 1.7, ±162%) and SSTA from –1.9 to 1.7 (–0.3 ± 0.9 or ±270% variability).

The 6-year time series show a covariation of discharge and precipitation (R^2 = 0.22; $p < 0.001$ for monthly averages) with major peaks normally concentrated in the austral spring (October–

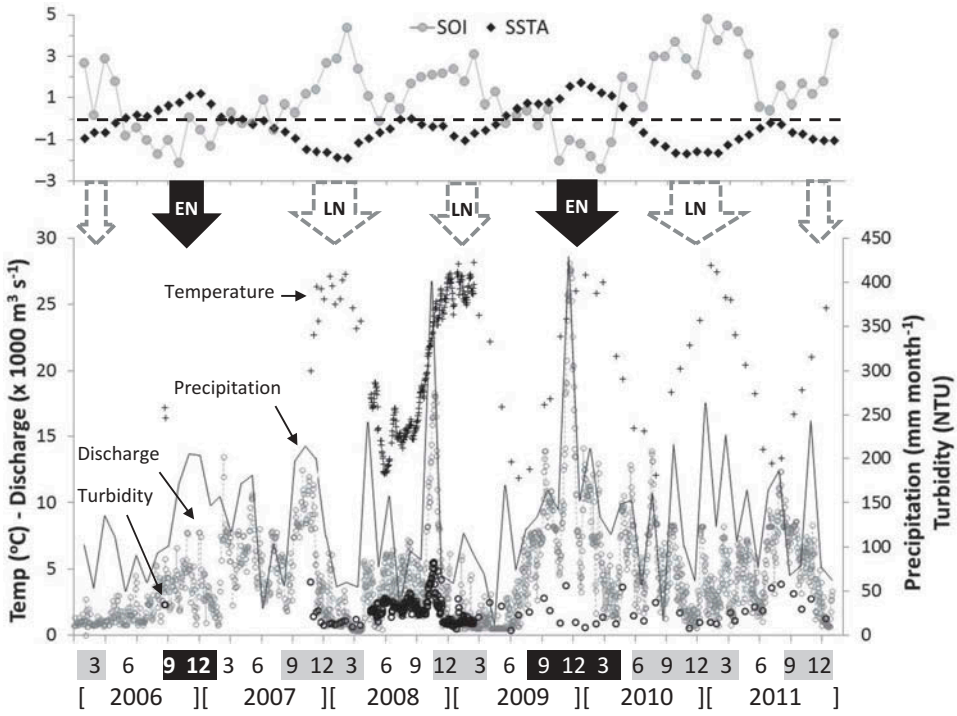

Fig. 3 Variability of hydro-meteorological parameters and ENSO indexes (SOI: southern oscillation Index; SSTA: sea surface temperature anomaly for region 3.4). El Niño (EN, solid black arrows) and La Niña episodes (LN, dashed arrows) are indicated in the time scale (highlighted black and grey months, respectively).

December, less marked in 2010), and lowest values in the winter (June–August). Turbidity also follows this pattern with highest values during discharge peaks.

In the case of SOI and SSTA, two warm El Niño episodes with negative SOI and highest SSTA are identified; one moderate covering September 2006–January 2007 (average SOI: –1.0; SSTA: 0.9) and another strong from July 2009 to April 2010 (SOI: –1.6; SSTA: 1.3). The contrasting cold La Niña episodes of highest SOI and lowest SSTA are observed five times, moderate in January–March 2006 (SOI: 1.9; SSTA: –0.7), strong in August 2007–April 2008 (SOI: 1.9; SSTA: –1.3), moderate in December 2008–March 2009 (SOI: 2.0; SSTA: –0.8), strong in June 2010–April 2011 (SOI: 3.2; SSTA: –1.3) and a moderate episode at the end of the series in September–December 2011 (SOI: 2.2; SSTA: –1.0). These episodes are formally recognized by the NOAA operational definitions of El Niño–La Niña events: 3-month average SSTA greater than or equal to (EN) and lower than or equal to (LN) 0.5°C for five successive overlapping quarters (Climate Prediction Centre 2013).

There is a connection of precipitation and discharge with ENSO, especially during the strong 2009/10 EN event, and of lowest values during LN, but considering the 6-year time series the relationships are very weak (inverse with SOI and direct with SSTA), only significant for SSTA-discharge (SSTA-FW, $R^2 = 0.12$; $p = 0.002$). Considering monthly average SSTA-discharge correlations, significant positive relationships are obtained for both EN years 2006 ($R^2 = 0.79$; $p < 0.001$) and 2009 ($R^2 = 0.72$; $p < 0.001$), with non-significant results for 2008 ($R^2 = 0.30$; $p = 0.065$), 2011 ($R^2 = 0.20$; $p = 0.139$), 2010 ($R^2 = 0.18$; $p = 0.169$) and especially 2007, which suggest a negative trend ($R^2 = 0.14$; $p = 0.236$).

The spectral analysis of SSTA and log-transformed Uruguay River discharge data shows some comparable energy (variance) maxima (Fig. 4). River discharge spectra display the presence of three peaks at a frequency of 0.028, 0.055 and 0.08 (approx. 3, 1.5 and 1 year), whereas SSTA show two coincident variance maxima (0.028 and 0.055). Evaluation of the SSTA-discharge coherence shows higher values for the 3-year peak relative to the 1.5-year maxima (square coherence: 0.62 *vs* 0.54).

The single most significant feature uncoupled to ENSO is the large precipitation and discharge peaks of November 2008 coincident with neutral

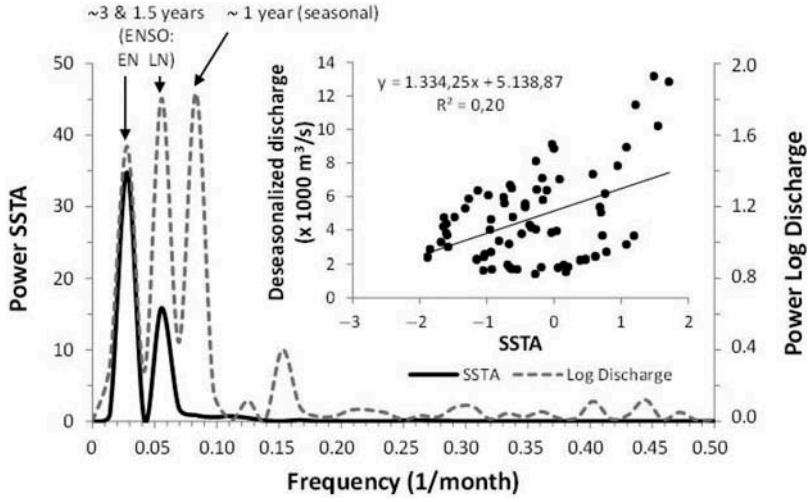

Fig. 4 Spectral analysis showing main variances of log-transformed freshwater discharges and sea-surface temperature anomalies (SSTA), and correlation of deseasonalized discharge data and SSTA.

conditions, followed by a moderate cold episode. This peak is an extreme value of the annual cycle, which could be extracted by deseasonalizing the data (see Method Section). Once the seasonal variability is removed, the SSTA-discharge correlation improves ($R^2 = 0.20$; $p < 0.001$; Fig. 4).

The variability of several water quality parameters is associated with discharge patterns (Fig. 5). Turbidity displays a significant positive correlation with river flow ($R^2 = 0.57$; $p < 0.001$), whereas the quite conservative pH values (7.4 ± 0.3 or ±4.2%) show an opposite pattern ($R^2 = 0.53$). In contrast, conductivity (62 ± 12 µS cm^{-1}; ±19%) and dissolved oxygen (8.2 ± 1.2 mg L^{-1}; ±15%) show no significant relationship with water discharge (Fig. 5). The settling material collected by the traps also shows variability associated with the river regime. The particle flux is relatively high and variable (75 ± 64 g m^2 d^{-1}; ± 86%), positively correlated with turbidity (R^2 = 0.31) and increases with river flow ($R^2 = 0.36$). The TOC content of the settling material (3.2 ± 0.8%; ±25%) does not show any significant pattern, whereas the C/N ratio (11.5 ± 0.7; ±6%) suggests a non-significant positive trend with river flow (10–11 to 12–13; $R^2 = 0.09$; Fig. 5).

The combined effect of increasing river discharges and turbidity results in a strong pattern of highest solid load fluxes during river floods. Figure 6 presents the relationship of sediment load obtained from turbidity (mg L^{-1} = NTU × 1.21) and river discharge (note logarithmic scale). The data fit a potential curve ($y = 0.164x^{1.348}$; $R^2 = 0.92$), as is normally observed for total suspended solids-discharge correlations (Dodds and Whiles 2004). These results indicate that under normal flow conditions (2500–5000 m^3 s^{-1}) the solid load ranges from approx. 6000 to 16 000 t d^{-1} and can reach >100 000 t d^{-1} during extreme floods like those of November 2008 and 2009.

5 DISCUSSION

The influence of ENSO events on the precipitation and freshwater discharge of the Uruguay River observed in 2006/07, and particularly during the 2009/10 highest peak, is consistent with previous reports which indicate that ENSO timescale variability with characteristic 3.5- and 6-year components associated with Pacific SSTA is most marked in this river (Robertson and Mechoso 1998, Krepper *et al.* 2003). The variance maxima at 3 and 1.5 years observed in the spectral analysis of water discharge (Fig. 4) is consistent with similar peaks obtained in the SSTA spectra, i.e. two warm and five cold episodes, but the 3-year cycle show higher coherence. A similar 3.3-year periodicity for El Niño has been previously reported for the Paraná River (Depetris *et al.* 1996), but the 1.5-year variability component associated with LN cold episodes has not been recognized previously in the Río de la Plata Basin.

Superimposed on the ENSO inter-annual variability, the seasonal pattern of low summer-autumn waters and highest spring discharges is very significant, with a single, most significant precipitation and discharge peak in November 2008, coincident with neutral ENSO conditions and the beginning of a moderate

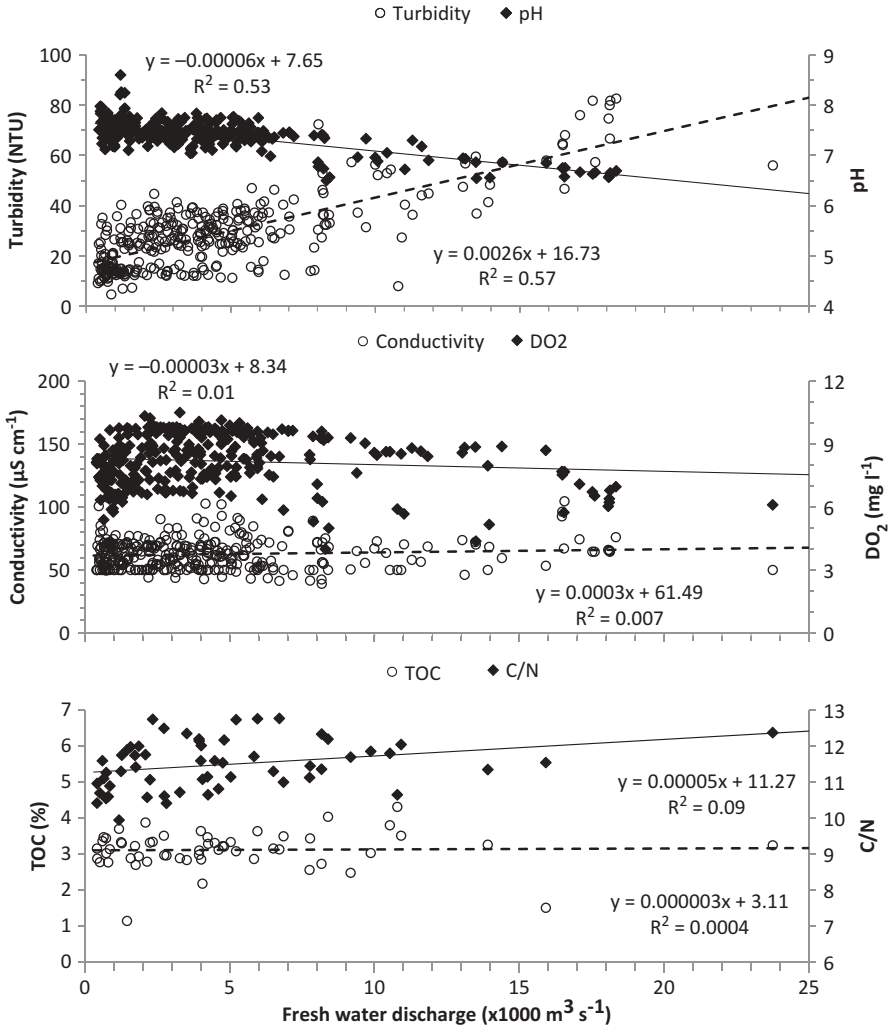

Fig. 5 Regressions between multi-parametric (turbidity, pH, Conductivity, Dissolved Oxygen) and sediment trap-derived water quality data (TOC, C/N ratio) and river flow.

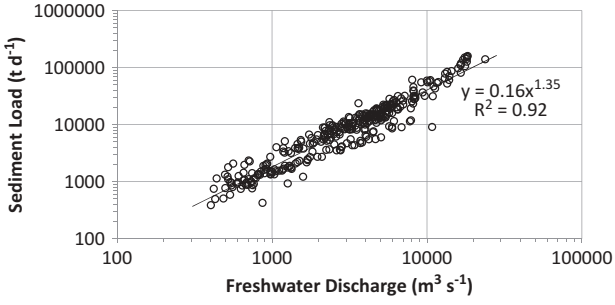

Fig. 6 Correlation of sediment load obtained from turbidity and river flow (note logarithmic scale).

La Niña episode. During strong ENSO events the seasonal pattern of spring discharge maxima is either accentuated (i.e. EN 2009/10) or attenuated (i.e. LN 2010/11). The improvement of the weak SSTA-freshwater discharge correlation observed for the whole 2006–2011 time series when the seasonal variability is removed (R^2 = 0.12 to 0.20), agrees with previous results calculated for the Uruguay River for shorter time scales for monthly SSTA-discharges for 2000–2002 (R^2 = 0.26; Nagy *et al.* 2008).

The observed variation of water quality parameters with river discharge basically reflects the enhanced erosion and transport of suspended material (turbidity and particle fluxes increase) and dilution with rainwater during high waters (pH decrease). The significant positive regression of turbidity and river flow (approx. 10–20 to >70 NTU; Fig. 5) reflect enhanced solid transport capacity, as has been observed in other rivers (Kusimi 2008). The flux of material collected by the traps also increases with higher discharges and correlates with turbidity reflecting the transport of eroded material during river floods. The organic content

of the particulated material does not show any significant trend during the three-times increase of the vertical particle flux (approx. 40 to >100 g m^2 d^{-1}) or >20-times rise of sediment load of the river (2000–40 000 t d^{-1}) with increasing discharge. The slight rise insinuated by C/N ratios with water discharge (Fig. 5) reflects the shift from autochthonous to allochthonous inputs in the river, i.e. from phytoplankton to terrestrial detritus as the river regime evolves from low, clear waters with sluggish currents in the summer when phytoplankton blooms, to high, turbid waters with strong currents transporting terrestrial matter in spring. Considering C/N ratios of 6.6 and 16 as end members for plankton and terrestrial detritus, respectively (Skorupka *et al.* 2003), the average rise of C/N ratios of the trap material (10.5 to ~12) represents a 41–57% increase of the terrestrial signal (36–66% for extreme 10–12.8 C/N ratios).

The inverse relationship observed for pH and river flow reflect the dilution with rainwater, which typically present acidic pH due to the carbon dioxide-carbonic acid equilibrium, i.e. pH = 5.6 in background sites of northeast Uruguay (Zunckel *et al.* 2003). Considering an average pH of 7.5 for normal Uruguay River flow regimes (pH: 7.3–7.7 for 2500–5000 m^3 s^{-1}; Fig. 5) and 5.6 for unpolluted rainwater as end members, a simple linear dilution model indicates that the extreme pH value of 6.6 measured for discharges >18 000 m^3 s^{-1} corresponds to a 47% rainwater contribution. The imbalance between this >3-times discharge increase (approx. 5000 *vs* 18 000 m^3 s^{-1}) and the ~approx. 50% rainwater contribution (i.e. two-times) is probably related to the partial buffering of rainwater acidity by the carbonate-bicarbonate system of the river which is typically enriched in calcium bicarbonate (Janiot and Molina 2001). The normally variable conductivity of rainwaters (<100 µS cm^{-1}; Sequeira and Lung 1995, García *et al.* 2007) relative to low, conservative Uruguay River values (approx. 50–70 µS cm^{-1}) appear to mask any significant association of this parameter with river flow increase during rain events.

The cubic relationship of the total sediment load and freshwater discharge indicate that most of the annual solid load of the Uruguay River is concentrated in October–November during episodic floods (>10 000 m^3 s^{-1}; Fig. 6), as has been observed in other world rivers (Moatar *et al.* 2006). During these events, sediment load scales an order of magnitude, i.e. from 4000–9000 to 50 000–70 000 t d^{-1} in 2008–2009. These results contrast with those reported for the El Niño-related largest flood on the Paraná River in 1982, when no net increase in the transport of suspended matter was observed relative to pre-ENSO loads(146 300 *vs* 180 548 t d^{-1} for 24 400 *vs* 13 952 m^3 s^{-1}; Depetris and Kempe 1990). This has been attributed to the filtering effect of the extensive wooded floodplain of the Paraná River. The three-times lower water discharge and limited floodplain of the Uruguay River which runs mostly along a deeper mainstream channel might partially explain the different patterns observed in both rivers.

6 CONCLUSIONS

Uruguay River hydro-meteorological parameters displayed significant (24–85%) seasonal and inter-annual variability throughout the 6-year time series. The seasonal pattern comprises basically spring maxima for precipitation, water discharge and turbidity, with lowest values in summer and winter. ENSO influence acts either reinforcing (2006/07 and 2009/10 El Niño) or attenuating the peaks (2006, 2008, 2009 and 2010/11, end-2011 La Niña). Spectral analysis of sea-surface temperature anomaly (SSTA) and Uruguay River discharge indicated variance maxima at approx. 3 years (higher coherence) and 1.5 years, with a seasonal approx. 1-year peak for discharge. Deseasonalized discharge data were significantly correlated to SSTA. Turbidity increased with water discharge due to enhanced erosion and sediment transport resulting in 1–2 orders of magnitude increase in the solid load during river floods. In contrast, pH displayed an inverse relationship reflecting the contribution of acidic rainwaters during major rain–discharge events. Settling particle fluxes increased with water discharge, but TOC contents of particles remained stable, whereas C/N ratios suggest an increasing pattern probably related to the intensification of terrestrial over autochthonous inputs during high waters.

Disclosure statement No potential conflict of interest was reported by the author(s).

REFERENCES

Almeira, G.J. and Scian, B., 2006. Some atmospheric and oceanic indices as predictors of seasonal rainfall in the Del Plata Basin of Argentina. *Journal of Hydrology*, 329, 350–359. doi:10.1016/j.jhydrol.2006.02.027

Barros, V., Clarke, R., and Silva Dias, P., 2005. Climate change in the La Plata Basin. Consejo Nacional de Investigaciones Científicas y Técnicas (CONICET). Project SGP II 057,

Trends in the hydrological cycle of the Plata basin: Raising awareness and new tools for water management. Inter American Institute on Global Change (IAI), 219 p.

Camilloni, I.A. and Barros, V.R., 2003. Extreme discharge events in the Paraná River and their climate forcing. *Journal of Hydrology*, 278, 94–106. doi:10.1016/S0022-1694(03)00133-1

Cardoso, A.O. and Silva Dias, P.L., 2006. The relationship between ENSO and Paraná River flow. *Advances in Geosciences*, 6, 189–193. doi:10.5194/adgeo-6-189-2006

Climate Prediction Centre, 2013. ENSO cycle: recent evolution, current status and predictions. Available from: www.cpc.ncep.noaa.gov [Accessed November 2013].

Colombo, J.C., *et al*., 2005. Sources, vertical fluxes, and accumulation of aliphatic hydrocarbons in coastal sediments of the Río de la Plata Estuary, Argentina. *Environmental Science & Technology*, 39, 8227–8234. doi:10.1021/es051205g

Colombo, J.C., *et al*., 2007. Vertical fluxes and organic composition of settling material from the sewage impacted Buenos Aires coastal area, Argentina. *Organic Geochemistry*, 38, 1941–1952. doi:10.1016/j.orggeochem.2007.07.005

Degens, E.T., Kempe, S., and Richey, J.E., 1991. Summary: biogeochemistry of major world rivers. *In*: E.T. Degens, S. Kempe, and J.E. Richey, eds. *Biogeochemistry of major world rivers*. New York: John Wiley & Sons, 323–347.

Depetris, P.J. and Kempe, S., 1990. The impact of the El Niño 1982 event on the Paraná River, its discharge and carbon transport. *Palaeogeography, Palaeoclimatology, Palaeoecology (Global and Planetary Change Section)*, 89, 239–244. doi:10.1016/0031-0182(90)90064-E

Depetris, P.J., *et al*., 1996. ENSO-controlled flooding of the Paraná River (1904-1991). *Naturwissenschaften*, 83, 127–129. doi:10.1007/BF01142177

Dodds, W.K. and Whiles, M.R., 2004. Quality and quantity of suspended particles in rivers: continent-scale patterns in the United States. *Environmental Management*, 33, 355–367. doi:10.1007/s00267-003-0089-z

Esteves, J.L., *et al*., 2000. The Argentine Sea: the Southeast South American shelf marine ecosystem. *In*: C. Sheppard, ed. *Seas at the millennium: an environmental evaluation*. Oxford: Elsevier, 749–771.

García, M.G., *et al*., 2007. Sources of dissolved REE in mountainous streams draining granitic rocks, Sierras Pampeanas (Córdoba, Argentina). *Geochimica et Cosmochimica Acta*, 71, 5355–5368. doi:10.1016/j.gca.2007.09.017

García, N.O. and Vargas, W.M., 1998. The temporal climatic variability in the Río de la Plata Basin displayed by the river discharges. *Climatic Change*, 38, 359–379. doi:10.1023/A:1005386530866

Janiot, L.J. and Molina, D.A., 2001. Características fisicoquímicas del Río Uruguay en su curso inferior. III Seminario sobre Calidad de las Aguas y Contaminación. Publicaciones de la Comisión Administradora del Río Uruguay, p. 7–12.

Krepper, C.M., García, N.O., and Jones, P.D., 2003. Interannual variability in the Uruguay River Basin. *International Journal of Climatology*, 23, 103–115. doi:10.1002/joc.853

Kusimi, J.M., 2008. Analysis of sedimentation rates in the Densu River channel: the result of erosion and anthropogenic activities in the Densu Basin. *West African Journal of Applied Ecology*, 14, 1–14.

Labat, D., 2008. Wavelet analysis of the annual discharge records of the world's largest rivers. *Advances in Water Resources*, 31, 109–117. doi:10.1016/j.advwatres.2007.07.004

Moatar, F., *et al*., 2006. The influence of contrasting suspended particulate matter transport regimes on the bias and precision of flux estimates. *Science of the Total Environment*, 370, 515–531. doi:10.1016/j.scitotenv.2006.07.029

Nagy, G.J., *et al*., 2008. Rio de la Plata estuarine system: relationship between river flow and frontal variability. *Advances in Space Research*, 41, 1876–1881. doi:10.1016/j.asr.2007.11.027

Pasquini, A.I. and Depetris, P.J., 2007. Discharge trends and flow dynamics of South American rivers draining the southern Atlantic seaboard: an overview. *Journal of Hydrology*, 333, 385–399. doi:10.1016/j.jhydrol.2006.09.005

Pasquini, A.I. and Depetris, P.J., 2010. ENSO-triggered exceptional flooding in the Paraná River: where is the excess water coming from? *Journal of Hydrology*, 383, 186–193. doi:10.1016/j.jhydrol.2009.12.035

Robertson, A.W. and Mechoso, C.R., 1998. Interannual and decadal cycles in river flows of southeastern South America. *Journal of Climate*, 11, 2570–2581. doi:10.1175/1520-0442(1998)011<2570:IADCIR>2.0.CO;2

Sequeira, R. and Lung, F., 1995. A critical data analysis and interpretation of the pH, ion loadings and electrical conductivity of rainwater from the territory of Hong Kong. *Atmospheric Environment*, 29, 2439–2447. doi:10.1016/1352-2310(95)00161-Q

Skorupka, C.N., *et al*., 2003. Variación espacial de carbono y nitrógeno en sedimentos del Río de la Plata. *In*: V *Jornadas Nacionales de Ciencias del Mar*, 8–12 de Diciembre. Mar del Plata: National University of Mar del Plata - National Institute of Fisheries Research and Development, p. 175.

Zunckel, M., Saizar, C., and Zarauz, J., 2003. Rainwater composition in northeast Uruguay. *Atmospheric Environment*, 37, 1601–1611. doi:10.1016/S1352-2310(03)00007-4